

Fig. 2. Continuous tuning curve measured for the cw Raman laser. The pump frequency tuning is shown relative to 378440.00 GHz, as measured by a Burleigh wavemeter with 10-MHz resolution. Note that at point A, there is some coexistence of the rotational (Rot.) and vibrational (Vib.) Stokes. At point B, we measure the power dependence, as shown in Fig. 3, below.

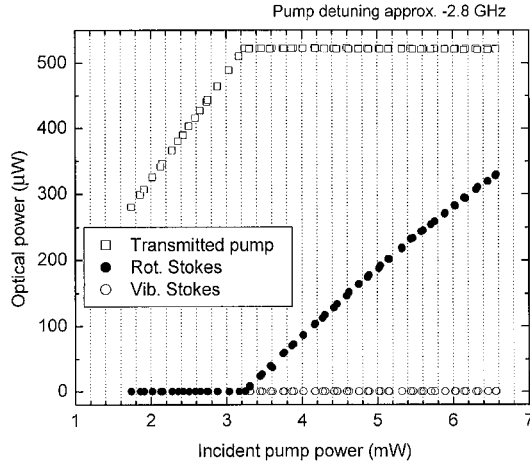


Fig. 3. Plot of the rotational Stokes power and transmitted pump power as a function of the incident pump power. The growth of the Stokes power and clamping of the pump power that can be seen are similar to what was observed for the vibrational cw Raman laser.²

where λ_p and λ_s are the wavelengths of the pump and Stokes, respectively. The Raman gain, pressure broadened at a high pressure of 10 atm, exhibits a homogeneous Lorentzian line shape for both the vibrational and the rotational transitions. The Raman plane-wave gain coefficient α associated with a cavity mode of the Stokes can then be modified as

$$\alpha(\delta\nu_p) = \alpha_0 \frac{(\Gamma/2)^2}{\Delta(\delta\nu_p)^2 + (\Gamma/2)^2},$$

where α_0 is the Raman plane-wave gain coefficient at the gain line center and Γ is the FWHM Raman gain linewidth. At a temperature of 300 K, a H_2 pressure of 10 atm, and a pump wavelength of 792 nm, we calculate that, for vibrational Raman transition $Q_{01}(1)$, $\alpha_{0v} = 1.5 \times 10^{-11}$ m/W (Ref. 9) and $\Gamma_v = 0.5$ GHz,¹⁰ while for rotational Raman transi-

tion $S_{00}(1)$, $\alpha_{0r} = 0.54 \times 10^{-11}$ m/W (Refs. 11–13) $\Gamma_r = 1.02$ GHz.¹⁴ Using these parameters, in Fig. 4(a) we plot theoretically the Raman plane-wave gain coefficients associated with the vibrational and rotational Stokes cavity modes as functions of the pump frequency tuning.

The tuning curve observed in Fig. 2 can now be qualitatively explained. Because of the homogeneous nature of the Raman transitions, the Stokes mode with the largest net gain will oscillate. Based on this rule, we calculate the powers of the transmitted pump, the vibrational Stokes, and the rotational Stokes as functions of the pump frequency tuning, using the theory given in Ref. 4, and plot them in Fig. 4(b). One can see a qualitative agreement between measurement and theory, except that only an ~ 6 -GHz range of the pump

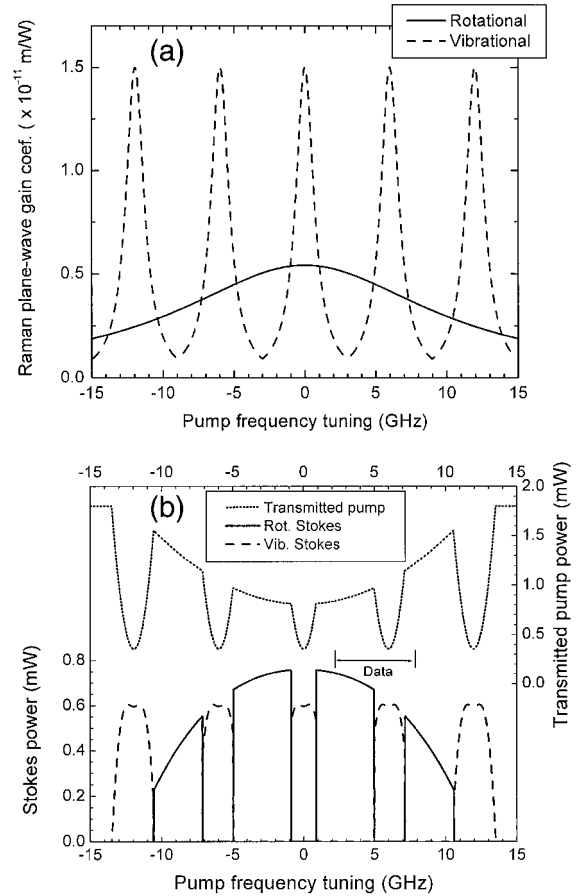


Fig. 4. (a) Theoretical plot of the Raman plane-wave gain coefficients of the rotational and vibrational transitions as functions of pump frequency tuning. The plot shows higher peak gain for the vibrational transition but wider tuning linewidth for the rotational transition in our double-resonance cavity. The cavity resonances of both Stokes are assumed to be at the gain line center when the relative pump frequency is zero [i.e., $\Delta(0) = 0$]. (b) Based on these gain profiles, the power of the transmitted pump, the rotational Stokes, and the vibrational Stokes are calculated as functions of pump tuning. The parameters used for the calculation are mirror reflectance, 0.9999; mirror absorptions, 40 parts in 10^6 at all wavelengths and both mirrors; and input pump power, 5 mW. The range shown is in qualitative agreement with the measured data presented in Fig. 2.

frequency can be tuned in the measurement because of the limited output range of the locking servo for the cavity piezoelectric transducer of 0–150V, which corresponds to a physical tuning range of $\sim 1.2 \mu\text{m}$ of the piezoelectric transducer tube between the cavity mirrors.

Two phenomena in the laser's tuning behavior are noted. First, in spite of its smaller gain, the rotational Stokes can emit at higher power than the vibrational Stokes [see Fig. 2 or the middle range in Fig. 4(b)]. This counterintuitive effect is due to the smaller Raman shift of the rotational transition. In other words, more energy from each pump photon is transferred to the rotational Stokes photon than to the vibrational Stokes photon. Second, there is some coexistence of the two Stokes when the pump frequency is tuned to the switching point (see point A in Fig. 2). We believe that this coexistence is due to the slight inhomogeneity of the Raman gain (caused by Doppler broadening).

We did not quantitatively compare the theoretical calculation with the experimental data because we found that the interference effect between the two surfaces of the HFC mirrors caused significant modulation of the mirrors' effective reflectance as a function of the laser's frequency (for example, the results of our cavity ringdown measurements showed as large as 20% variation). This effect thus adds background modulation to the cavity-transmitted pump and Stokes powers as their frequencies are tuned and makes quantitative comparison difficult. The same problem is common in cavity ringdown spectroscopy (see, for example Ref. 15). To compare the theory with the data quantitatively, one should use mirrors with back surfaces that are wedged and (or) antireflection coated.

The fact that the rotational Raman shift is considerably smaller than the vibrational transition (586.9 versus 4155 cm^{-1} in H_2) can be advantageous. First, for the rotational Raman transition, the bandwidth of a single-wavelength mirror coating can be sufficient to cover both the pump and Stokes wavelengths, whereas the double-wavelength coating required for the vibrational cw Raman laser is far more expensive and difficult to manufacture. Second, the continuous tuning range of the Stokes emission near four times threshold is $\Gamma(\lambda_s/\lambda_p - 1)^{-1}$,³ and thus a rotational Raman laser can have a much wider continuous tuning range ($>21 \text{ GHz}$ for the $792\text{--}830\text{-nm}$ transition if the cavity length change has no physical limitation) than a vibrational Raman laser ($\sim 1 \text{ GHz}$ for the $792\text{--}1180\text{-nm}$ transition). Third, the thermo-optic effects caused by heat deposition in the Raman gas are less of a problem for the rotational Raman transition because of its smaller photon energy shift, whereas it has been

observed that in the high-power vibrational Raman laser thermo-optic effects can lower the conversion efficiency and cause instabilities.^{16,17}

In summary, we have reported a diode-pumped cw Raman laser with rotational Stokes emission. In many fields, such as laser spectroscopy and atomic physics, a small shift of an existing laser wavelength is often necessary to match the preferred wavelength exactly. The rotational cw Raman laser provides a new technique that is useful in such applications.

This material is based on work supported by the National Science Foundation under grant 0097222. J. Carlsten's e-mail address is carlsten@physics.montana.edu.

References

1. J. K. Brasseur, K. S. Repasky, and J. L. Carlsten, *Opt. Lett.* **23**, 367 (1998).
2. L. S. Meng, K. S. Repasky, P. A. Roos, and J. L. Carlsten, *Opt. Lett.* **25**, 472 (2000).
3. J. K. Brasseur, P. A. Roos, L. S. Meng, and J. L. Carlsten, *J. Opt. Soc. Am. B* **17**, 1229 (2000).
4. J. K. Brasseur, P. A. Roos, K. S. Repasky, and J. L. Carlsten, *J. Opt. Soc. Am. B* **16**, 1305 (1999).
5. For a definition of the notation $Q_{01}(1)$ and $S_{00}(1)$, see Table 1 in R. W. Minck, E. E. Hagenlocker, and W. G. Rado, Ford Motor Company Tech. Rep. SL66-24 (Ford Motor Company, Detroit, Mich., March, 1966).
6. Stimulated pure rotational Raman scattering with high-power pulsed lasers was first observed in gaseous deuterium by R. W. Minck, E. E. Hagenlocker, and W. G. Rado, *Phys. Rev. Lett.* **17**, 229 (1966).
7. R. W. Drever, J. L. Hall, F. V. Kowalski, J. Hough, G. M. Ford, A. J. Munley, and H. Ward, *Appl. Phys. B* **31**, 97 (1983).
8. G. V. Venkin, Yu. A. Il'inskii, and G. M. Mikheev, *Sov. J. Quantum Electron.* **15**, 395 (1985).
9. W. K. Bischel and M. J. Dyer, *J. Opt. Soc. Am. B* **3**, 677 (1986).
10. W. K. Bischel and M. J. Dyer, *Phys. Rev. A* **33**, 3113 (1986).
11. Although no direct measurement was performed on this gain coefficient, we calculated α_{0r} by use of formulas and data from J. L. Carlsten and R. G. Wenzel, *IEEE J. Quantum Electron.* **19**, 1407 (1983).
12. See also R. W. Carlson and W. R. Fenner, *Astrophys. J.* **178**, 551 (1972).
13. See also M. R. Perrone, V. Piccinno, G. De Nunzio, and V. Nassisi, *IEEE J. Quantum Electron.* **33**, 938 (1997).
14. G. C. Herring, M. J. Dyer, and W. K. Bischel, *Phys. Rev. A* **34**, 1944 (1986).
15. J.-W. Hahn, Y.-S. Yoo, J.-Y. Lee, J.-W. Kim, and H.-W. Lee, *Appl. Opt.* **38**, 1859 (1999).
16. L. S. Meng, P. A. Roos, K. S. Repasky, and J. L. Carlsten, *Opt. Lett.* **26**, 426 (2001).
17. J. Bienfang, W. Rudolph, P. A. Roos, L. S. Meng, and J. L. Carlsten, *J. Opt. Soc. Am. B* **19**, 1318 (2002).